



The sodium leak channel NALCN regulates cell excitability of pituitary endocrine cells

Hathaichanok Impheng, Céline Lemmers, Malik Bouasse, Christian Legros, Narawut Pakaprot, Nathalie C. Guérineau, Philippe Lory, Arnaud Monteil

► To cite this version:

Hathaichanok Impheng, Céline Lemmers, Malik Bouasse, Christian Legros, Narawut Pakaprot, et al.. The sodium leak channel NALCN regulates cell excitability of pituitary endocrine cells. *FASEB Journal*, 2021, 35 (5), pp.e21400. 10.1096/fj.202000841rr . hal-03188856

HAL Id: hal-03188856

<https://hal.science/hal-03188856>






Submitted on 2 Apr 2021

HAL is a multi-disciplinary open access archive for the deposit and dissemination of scientific research documents, whether they are published or not. The documents may come from teaching and research institutions in France or abroad, or from public or private research centers.

L'archive ouverte pluridisciplinaire **HAL**, est destinée au dépôt et à la diffusion de documents scientifiques de niveau recherche, publiés ou non, émanant des établissements d'enseignement et de recherche français ou étrangers, des laboratoires publics ou privés.

RESEARCH ARTICLE

The sodium leak channel NALCN regulates cell excitability of pituitary endocrine cells

Hathaichanok Impheng^{1,2} | Céline Lemmers^{1,3} | Malik Bouasse^{1,2} | Christian Legros⁴  | Narawut Pakaprot⁵  | Nathalie C. Guérineau^{1,2}  | Philippe Lory^{1,2}  | Arnaud Monteil^{1,2,3} 

¹IGF, Université de Montpellier, CNRS, INSERM, Montpellier, France

²LabEx 'Ion Channel Science and Therapeutics', Montpellier, France

³PVM, BCM, Université de Montpellier, CNRS, INSERM, Montpellier, France

⁴MITOVASC Institute, UMR CNRS 6015 - UMR INSERM U1083, Université d'Angers, Angers, France

⁵Department of Physiology, Faculty of Medicine Siriraj Hospital, Mahidol University, Bangkok, Thailand

Correspondence

Arnaud Monteil, IGF, Université de Montpellier, CNRS, INSERM, Montpellier, France.

Email: arnaud.monteil@igf.cnrs.fr

Present address

Hathaichanok Impheng, Department of Physiology, Faculty of Medical Sciences, Naresuan University, Phitsanulok, Thailand

Funding information

Fondation pour la Recherche Médicale (FRM), Grant/Award Number: DEQ20170336728; Laboratory of Excellence 'Ion Channel Science and Therapeutics'; Association Française contre les Myopathies (AFM), Grant/Award Number: 20151; Fondation Maladies Rares; Naresuan University (NU); French Ministry for Foreign Affairs

Abstract

Anterior pituitary endocrine cells that release hormones such as growth hormone and prolactin are excitable and fire action potentials. In these cells, several studies previously showed that extracellular sodium (Na^+) removal resulted in a negative shift of the resting membrane potential (RMP) and a subsequent inhibition of the spontaneous firing of action potentials, suggesting the contribution of a Na^+ background conductance. Here, we show that the Na^+ leak channel NALCN conducts a Ca^{2+} - Gd^{3+} -sensitive and TTX-resistant Na^+ background conductance in the GH₃ cell line, a cell model of pituitary endocrine cells. NALCN knockdown hyperpolarized the RMP, altered GH₃ cell electrical properties and inhibited prolactin secretion. Conversely, the overexpression of NALCN depolarized the RMP, also reshaping the electrical properties of GH₃ cells. Overall, our results indicate that NALCN is functional in GH₃ cells and involved in endocrine cell excitability as well as in hormone secretion. Indeed, the GH₃ cell line suitably models native pituitary cells that display a similar Na^+ background conductance and appears as a proper cellular model to study the role of NALCN in cellular excitability.

KEYWORDS

background conductance, extracellular Ca^{2+} , ion channels, resting membrane potential

Abbreviations: 2-APB, 2-Aminoethoxydiphenyl borate; Ca_v , voltage-gated calcium channel; eGFP, enhanced Green Fluorescent Protein; FDR, false discovery rate; GH, growth hormone; HP, holding potential; K_v , voltage-gated potassium channel; Na_v , voltage-gated sodium channel; NMDG, N-methyl-D-glucamine; PRL, prolactin; RMP, resting membrane potential; TRH, thyrotropin-releasing hormone; TRP, Transient Receptor Potential; TTX, tetrodotoxin; V_m , membrane Potential.

This is an open access article under the terms of the Creative Commons Attribution-NonCommercial-NoDerivs License, which permits use and distribution in any medium, provided the original work is properly cited, the use is non-commercial and no modifications or adaptations are made.

© 2021 The Authors. *The FASEB Journal* published by Wiley Periodicals LLC on behalf of Federation of American Societies for Experimental Biology.

1 | INTRODUCTION

Anterior pituitary cells are excitable cells and express a large panel of ion channels involved in electrical activity and subsequent hormone release.¹ This includes high (L-, N-, P/Q-, and R-types) and low (T-type) voltage-gated calcium channels (Ca_v), voltage-gated potassium channels (K_v), and calcium-activated potassium channels (SK, IK, BK). These cells also express high and low tetrodotoxin (TTX)-sensitive voltage-gated Na^+ (Na_v) channels.²⁻⁵ In addition to these conductances, several studies also revealed the existence of a TTX-resistant background inward current carried by Na^+ in primary corticotrophs, gonadotrophs, lactotrophs, melanotrophs, and somatotrophs as well as in immortalized pituitary cells.⁶⁻¹⁵ Indeed, a Na^+ background conductance was suggested to belong to a common core set of ionic currents between the different subtypes of anterior pituitary endocrine cells.¹ This current maintains a relatively depolarized resting membrane potential (RMP) as demonstrated by the membrane hyperpolarization when Na^+ is replaced by large organic monovalent cations such as N-methyl-D-glucamine (NMDG) or Tris or choline.⁶⁻¹⁵ However, the molecular identity of this background inward Na^+ current remains to be determined. An expected candidate to support this conductance is the Na^+ leak channel NALCN, a four-domain ion channel related to Na_v and Ca_v channels.¹⁶ This channel was found to conduct a Gd^{3+} -sensitive and TTX-resistant Na^+ background conductance in several types of neurons from different species and its knockout or knockdown induced a membrane hyperpolarization.¹⁷⁻²⁵ Conversely, a gain-of-function mutation of NALCN resulted in a more depolarized RMP and an increase in the firing frequency of mouse deep mesencephalic nucleus neurons.²⁶ In the present study, we used the pituitary GH₃ cell line model to examine the contribution of NALCN in the previously described TTX-resistant Na^+ background conductance in this cell type.^{6,10-12} Our results showed that, in addition to NALCN, GH₃ cells endogenously express the other known components of the “NALCN channelosome” referred to as UNC79, UNC80, and FAM155A (also referred to as NLF-1). These components favor NALCN expression level, surface expression and function.²⁷ Genetic manipulation of the NALCN expression level was then set up and coupled to electrophysiological recordings. This led us to demonstrate that NALCN is a functional Na^+ leak channel in GH₃ cells and significantly contributes to their RMP and electrical activity as well as prolactin (PRL) secretion. Thus, our work provides the molecular basis of a background Na^+ current previously described in anterior pituitary endocrine cells. Overall, our data suggest that GH₃ cells represent a reliable cell model to study NALCN function/dysfunction in cell excitability.

2 | MATERIALS AND METHODS

2.1 | DNA constructs

The cloning of the human complementary DNA (cDNA) encoding wild-type NALCN was previously described.²⁸ Subcloning of the NALCN-encoding cDNAs in the lentiviral plasmid pLV-EF1 α -IRES-Neo, a gift from Tobias Meyer (Addgene #85139), was performed using standard molecular biology techniques. The eGFP was used as a control for the overexpression experiments. A microRNA-adapted shRNA based on miR-30 for specific NALCN silencing cloned in the lentiviral pGipz plasmid and targeting the 5'-GCAACAGACTGTGGCAATT-3' region of the rat NALCN-encoding RNA was obtained from a commercial source (Dharmacon #V2LMM_90196). A non-silencing control was used in our experiments (Dharmacon #RHS4346). Both controls for overexpression and knockdown displayed identical results in every experiment and are henceforth be referred to as Control.

2.2 | Cell culture

Rat pituitary GH₃ cells (ATCC[®] CCL-82.1[™]) were grown in Ham's F-12K (Kaighn's) medium (Thermo Fisher Scientific; #21127022) supplemented with 2.5% dialyzed fetal calf serum (Thermo Fisher Scientific; #10270106), 15% dialyzed horse serum (Thermo Fisher Scientific; #16005012), and 1% penicillin/streptomycin (Thermo Fisher Scientific; #15140122) at 37°C in a humidified atmosphere of 5% CO₂-95% air. The cells were passed once a week (split 1:3) with one additional feeding between passages.

2.3 | Lentivirus production and cell transduction

HIV-1 derived lentiviral particles were produced in HEK-293T cells and titrated as described.²⁹ GH₃ cells with 70%-80% of confluency were transduced with lentivirus (24 μg of P24) in 35 mm culture dishes then selected with G418 (700 $\mu\text{g}/\text{mL}$; Sigma-Aldrich #A1720) or puromycin (5 $\mu\text{g}/\text{mL}$; Sigma-Aldrich #P8833) for 1 month. The selection process resulted in the obtention of different cell lines: Control GH₃ cells, NALCN- (ie, knockdown) GH₃ cells and NALCN+ (ie, overexpression) GH₃ cells, referred to as Control, NALCN-, and NALCN+ in the text and the figures.

2.4 | Immunoblotting

Cells were lysed on ice for 20 minutes with NP-40 buffer containing 10 mmol/L Tris-HCl, pH 7.4, 120 mmol/L

NaCl, 1% NP-40, and proteases inhibitors (Roche Applied Science #04693124001). Cell lysates were spun at 10,000 g for 30 minutes at 4°C. Sixty micrograms of proteins were mixed with a 4x Laemmli buffer and then loaded on SDS-PAGE. Proteins resolved onto 4%-20% polyacrylamide gels (Bio-Rad #4561096) were transferred to Hybond C nitrocellulose membranes (GE Healthcare; #10600016). Membranes were immunoblotted with primary antibodies (rabbit anti-NALCN, 1:1000²⁸; rabbit anti- α -actinin, clone D6F6, 1:3000, Cell Signaling #6487), and then, with anti-rabbit horseradish peroxidase (HRP)-conjugated secondary antibody (1:10 000, GE Healthcare #NA934). Immunoreactivity was detected with an enhanced chemiluminescence substrate for detection of HRP (SuperSignal West Pico Chemiluminescent Substrate, Thermo Fisher Scientific #34080).

2.5 | Determination of prolactin (PRL) levels release

GH₃ cells (1×10^6 viable cells) were cultured in 6-well plates with 2 mL of medium/well. After a 4-day preculture (~90% confluency), the culture medium was changed into serum-free Ham's F-12K (Kaighn's) medium (Thermo Fisher Scientific #21127022). Cells were treated with thyrotropin releasing hormone, 100 nmol/L (TRH; Sigma-Aldrich #P1319) when indicated. A 100 μ L of cell supernatant was collected for prolactin (PRL) measurements at indicated times. The levels of prolactin in the supernatant were determined by rat-specific Enzyme Immunometric Assay (Bertin Technologies #A05101) according to the manufacturer's protocol. Cell protein was determined using the BCA protein assay kit (Thermo Fisher Scientific #23225). The results were expressed as ng of PRL per mg of total cellular protein after protein extraction.

2.6 | Electrophysiological recordings

Macroscopic currents were recorded at room temperature using an Axopatch 200B amplifier (Molecular Devices). Borosilicate glass pipettes (Sutter Instrument Co #BF150-86-15) had a resistance of 3 to 5 M Ω when filled with an internal solution containing (in mmol/L): 150 K-Gluconate, 10 NaCl, 5 HEPES, 1.1 EGTA (pH adjusted to 7.34 with NaOH, ~300 mOsm) with freshly added 0.6 GTP and 3 ATP before use. The extracellular solution contained (in mmol/L): 142.6 NaCl, 5.6 KCl, 2 CaCl₂, 0.8 MgCl₂, 5 Glucose, and 10 HEPES (pH adjusted to 7.35 with NaOH, ~310 mOsm). All the chemicals were purchased from Sigma-Aldrich. When indicated, extracellular Na⁺ was replaced with N-Methyl-D-glucamine (NMDG, Sigma-Aldrich #M2004) at the

same concentration. The recording chamber was constantly perfused (~100 μ L/min) with the control (Na⁺-containing) solution using a gravity-driven homemade perfusion device, which allowed extracellular medium change and drug application. TTX and Gd³⁺ were purchased from Latoxan (#L8503) and Sigma-Aldrich (#G7532), respectively. Spiking cells were referred to as cells exhibiting spontaneous action potential. Conversely, silent cells were referred to as cells that do not exhibit any spontaneous electrical activity.

2.7 | Quantitative PCR (qPCR)

Total RNA was extracted from cell cultures and rat tissues using the RNeasy Plus universal mini kit (Qiagen #74134). One μ g of total RNA was reverse transcribed to cDNA using the iScript kit (Bio-Rad #1708891) according to the manufacturer's protocol. Reverse transcribed products were diluted 10 times with H₂O and stored at -20°C until use. Real-time PCR was performed in 384 well plates in a final volume of 10 μ L using SYBR Green dye detection on the LightCycler480 system (Roche-Diagnostic#04887352001). The primer pairs were designed using the Primer 3 input software,³⁰ and their specificity and efficacy were experimentally validated. The Cq for individual genes was determined using the second Derivative Max tool of the LightCycler480 software. The relative RNA expression was calculated using the RNA helicase Ddx17 as a reference gene. Relative expressions were calculated using the $\Delta\Delta$ Cq method.³¹ Primers used in this study were: rat-NALCN-sense 5'-CAGAGGAGGAAGTTCGACAGG-3', rat-NALCN-antisense 5'-GCTTATTGGTTTGGGAGCTG-3', rat-Unc80-sense 5'-CTCTGTGGATCGCCTGTCTT-3', rat-Unc80-antisense 5'-GACAGCGCTGGTGAACCTTG-3', rat-Unc79-sense 5'-CAACCACACACGAACCTCCAC-3', rat-Unc79-antisense 5'-GCTGGCGGATGTCACAGT-3', rat-NLF1-sense 5'-CGGTGAAGTCCTGTCCTGA-3', rat-NLF1-antisense 5'-TTAACTGTGTGACTTCAAATACTGG-3', rat-Ddx17-sense 5'-AAGTTGATGCAGCTTGTGGA-3', rat-Ddx17-antisense 5'-GAAGTAGTCCGGTATCGTGAGC-3'.

2.8 | Data analysis

Data were analyzed using pCLAMP 9 (Molecular Devices) and Igor Pro 8 (WaveMetrics) softwares. Results are presented as mean \pm SEM or as violin plots; n is the number of cells and N the number of independent experiments. All the results presented in this study were obtained from at least three independent experiments. Statistical analyses were performed using GraphPad Prism (9.0). Depending on whether residuals followed or not a normal distribution, results were analyzed using either parametric or nonparametric tests. Additionally, depending on the experimental design,

they were analyzed using either *t*-test, or one-, two-, or three-ways ANOVA. *Cells types* (ie, *Control*, *NALCN*+, and *NALCN*-), and *Treatment* were used as between subjects' factors and *Time* as within subjects, repeated-measure factor. The test used in each dataset analysis is specified in the figure's legend. Post hoc analyses for multiple comparisons were performed with Benjamini, Krieger, & Yekutieli False Discovery Rate (FDR) corrections.

3 | RESULTS

3.1 | The GH₃ cell line endogenously expresses the NALCN channelosome-encoding mRNAs

To determine whether the sodium leak channel NALCN could be involved in the Na⁺ background conductance previously described in GH₃ cells, we first checked for its expression by RT-qPCR (Figure 1). We also extended our investigation to previously identified ancillary subunits. Indeed, several studies revealed the existence of at least three ancillary subunits named UNC79, UNC80 and FAM155A. These subunits interact with NALCN and are involved in the expression level, the cellular localization, the plasma membrane expression of the complex, as well as NALCN activation by the src kinase.²⁷ All the identified components of the NALCN channelosome were found to be expressed in GH₃ cells at the mRNA level. Unfortunately, we were not able to confirm this finding at the protein level because of the lack of commercially reliable antibodies with high sensitivity in our hands. However,

RT-qPCR results indicate that NALCN could be a candidate to contribute to excitability in this cell type. Therefore, we set up an experimental approach combining the manipulation of NALCN expression level with electrophysiological recordings using the patch-clamp technique to validate this hypothesis (Figure S1). In our experimental conditions, we were able to achieve a knockdown of ~ 80% for endogenous rat *Nalcn* in GH₃ cells at the mRNA level as assayed by RT-qPCR (NALCN- GH₃; Figure S2A). Conversely, heterologous overexpression of human NALCN was detected at both the mRNA and protein levels in this cell line (NALCN+ GH₃; Figure S2B,C).

3.2 | The NALCN expression level impacts the electrical activity of GH₃ cells

Similar to native endocrine pituitary cells, GH₃ cells are known to exhibit spontaneous Ca²⁺-dependent action potentials.^{32,33} This spontaneous electrical activity depends on a background Na⁺ conductance as it is fully abolished after the replacement of extracellular Na⁺ by large organic monovalent cations.^{6,10-12} Thus, we have performed recordings of the spontaneous electrical activity of our GH₃ cell lines using the patch-clamp technique in the whole-cell configuration (Figure 2). Spontaneous action potentials were detected in the three groups of GH₃ cells (ie, *Control*, *NALCN*+, and *NALCN*-; Figure 2A). Silent cells were also observed and we found the ratio of spiking versus silent cells to be different between the groups (Figure 2B). Indeed, the percentage of firing cell was clearly lower in both *NALCN*+

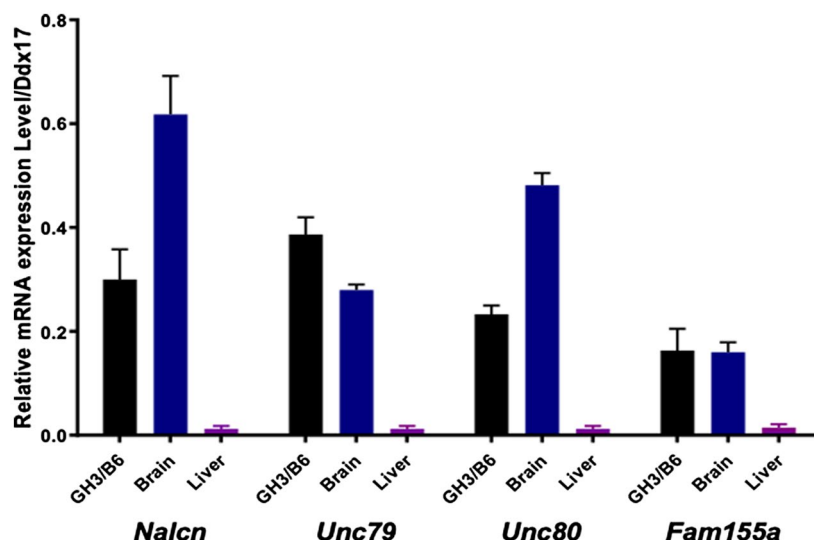


FIGURE 1 The GH₃ cell line endogenously expresses the NALCN channelosome-encoding mRNAs. RT-qPCR performed with total RNA extracted from GH₃ cells, rat adult brain and rat adult liver showing that *Nalcn*, *Unc79*, *Unc80*, and *Fam155a*, are expressed in GH₃ cells. Brain and liver were used as positive and negative controls, respectively. The gene encoding the RNA helicase Ddx17 was used as a housekeeping gene to determine the relative expression level (*Nalcn*: 0.3 ± 0.05; *Unc79*: 0.38 ± 0.03; *Unc80*: 0.23 ± 0.01; *Fam155a*: 0.16 ± 0.04; N = 4 independent experiments)

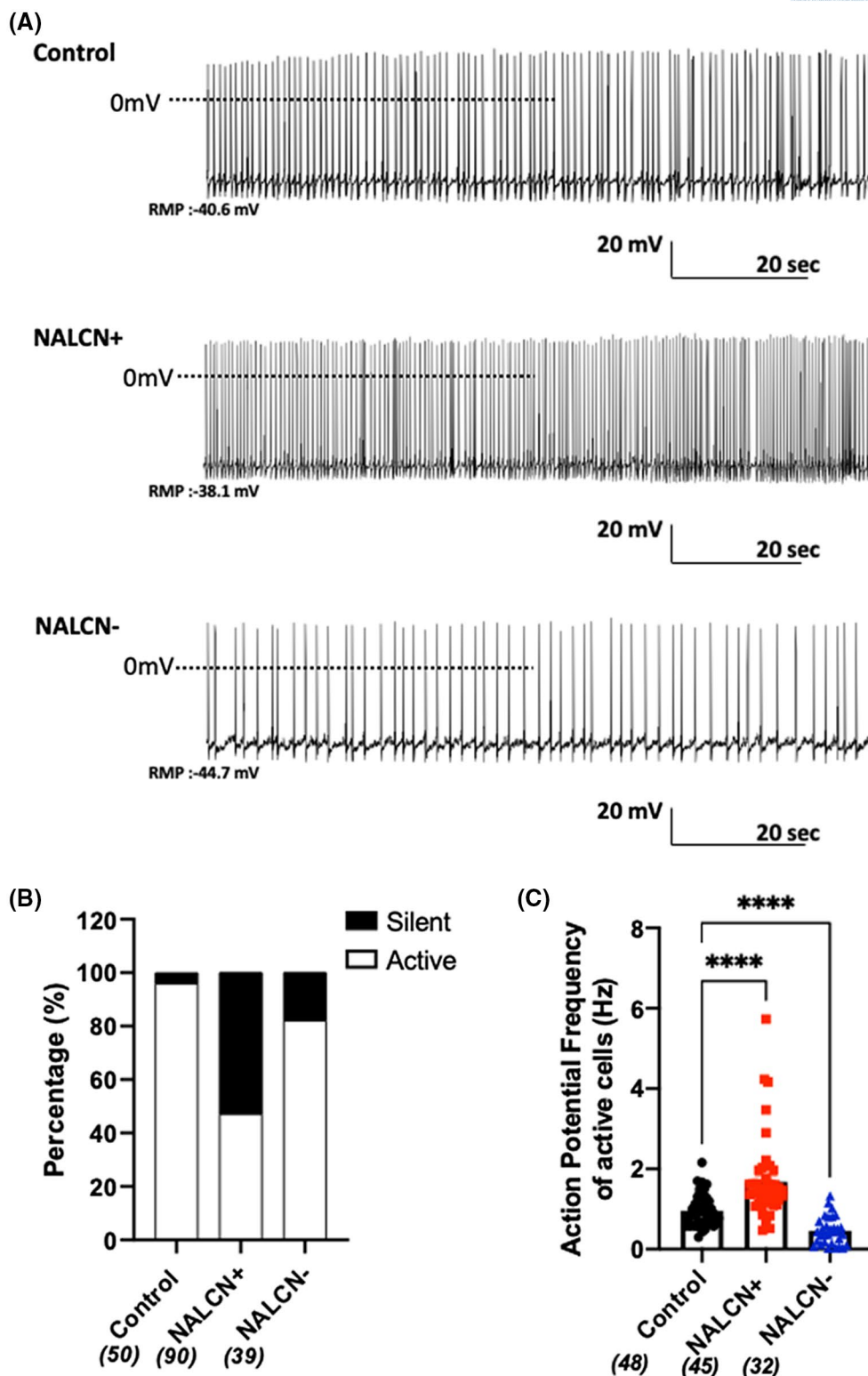


FIGURE 2 The NALCN expression level impacts the electrical activity of GH₃ cells. A, Representative traces of membrane potential recordings for the three conditions (eg, Control, NALCN+, and NALCN-). The RMP of representative traces represent the average RMP of spiking cells in each condition. B, Summary of the ratio of active versus silent cells for each condition. The percentage of active cell was notably lower in NALCN+ GH₃ cells and slightly lower in NALCN- GH₃ cells compared to the Control condition, respectively (Control: 95.9%, n = 50; NALCN+: 47.1%, n = 90; NALCN-: 82%, n = 39). C, Analysis of the firing frequency for GH₃ active cells in the three groups (control, NALCN+, and NALCN-). Results showed, respectively, significant higher and lower values for the NALCN+ and the NALCN- conditions compared to the Control condition, respectively (Control: 0.95 ± 0.05 Hz, n = 48; NALCN+: 1.68 ± 0.15 Hz, n = 45; NALCN-: 0.46 ± 0.06 Hz, n = 32). Statistical analysis: Kruskal-Wallis with FDR corrected post hoc tests; *****P* < .0001 compared to Control

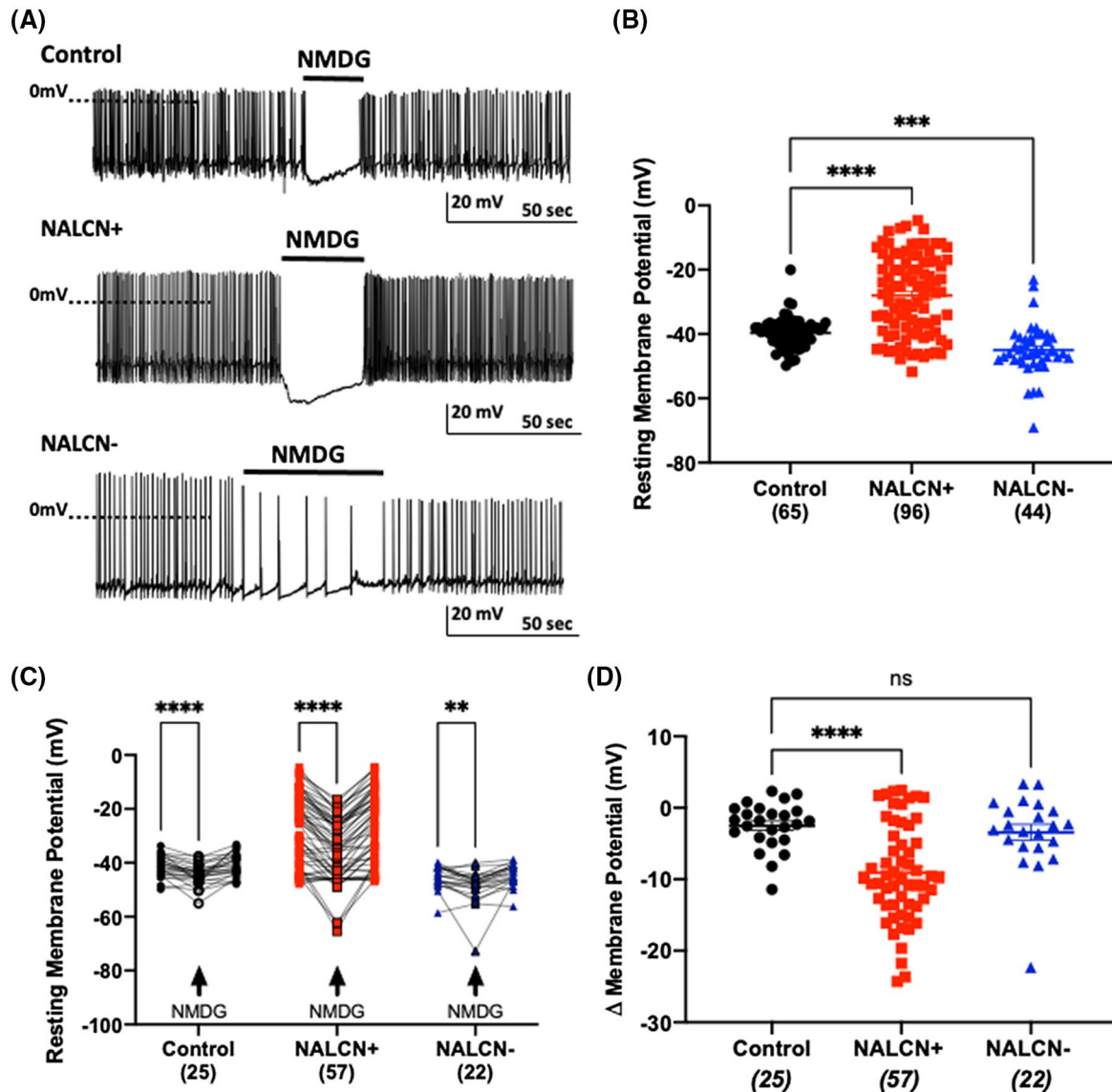


FIGURE 3 The NALCN expression level impacts the RMP of GH₃ cells. A, Representative traces of membrane potential recordings for the three conditions (Control, NALCN+, and NALCN-), during which extracellular Na⁺ was completely replaced with NMDG for 20 to 50 seconds (see black bars above each recording). Action potentials in GH₃ cells are carried by Ca²⁺.^{32,33} Extracellular Na⁺ removal resulted in the silencing of most of the cells and sometimes in a strongly reduced spiking activity. B, RMP in the presence of extracellular Na⁺ is more depolarized in the NALCN+ group and more negative in the NALCN- group compared to the Control condition (Control: -39.6 ± 0.5 mV, $n = 65$; NALCN+: -27.9 ± 1.2 mV, $n = 96$; NALCN-: -44.9 ± 1.1 mV, $n = 44$). Statistical analysis: Kruskal-Wallis with FDR corrected post hoc tests; *** $P < .001$, **** $P < .0001$ compared to Control. Because the determination of RMP cannot be reliably assessed by direct measurement on chart recordings of spontaneously firing cells, its mean value was calculated from the membrane potential distribution, as reported.⁵⁰ C, RMP variation in the presence and absence of extracellular Na⁺ (Control: -41.2 ± 0.8 vs -44.4 ± 0.7 mV, $n = 25$; NALCN+: -26.6 ± 1.7 vs -37.7 ± 1.5 mV, $n = 57$; NALCN-: -45.4 ± 0.8 vs -48.8 ± 1.3 mV, $n = 22$). Statistical analysis: for each cell type, paired t test; ** $P < .01$, **** $P < .001$, compared to Na⁺ 142.6 mmol/L. D, ΔRMP (ie, RMP with extracellular Na⁺ minus RMP in Na⁺-free condition) when NALCN is overexpressed compared of the control condition (Control: -2.0 ± 0.6 mV, $n = 25$; NALCN+: -9.0 ± 0.9 mV, $n = 57$; NALCN-: -3.4 ± 1.1 , $n = 22$). Statistical analysis: Kruskal-Wallis with FDR corrected post hoc tests; **** $P < .0001$ compared to Control

GH₃ and NALCN- GH₃ cells compared to the control condition (Control: 95.9%, $n = 50$; NALCN+: 47.1%, $n = 90$; NALCN-: 82%, $n = 39$). Interestingly, the firing frequency of spiking cells was found to be higher (~1.7-fold increase) when human NALCN was heterologously expressed and conversely to be lower (~1.8-fold decrease) than the

control group when rat NALCN was knocked down (Control: 0.95 ± 0.05 Hz, $n = 48$; NALCN+: 1.68 ± 0.15 Hz, $n = 45$, $P < .0001$; NALCN-: 0.46 ± 0.06 Hz, $n = 32$, $P < .0001$; Figure 2C). Altogether, these results demonstrated an important role of NALCN in regulating the spontaneous electrical activity of GH₃ cells.

3.3 | The NALCN expression level impacts the RMP of GH₃ cells

Since NALCN is involved in the regulation of the neuronal RMP,¹⁷⁻²⁶ further analysis of the membrane potential (Vm) in our cell lines was then carried out (Figure 3). Replacing extracellular Na⁺ by NMDG resulted in rapid and reversible membrane hyperpolarization and ending of spontaneous action potentials in the three conditions in the majority of the

cells (Figure 3A). The RMP in presence of extracellular Na⁺ was found to be more depolarized and less depolarized in NALCN+ GH₃ and NALCN- GH₃ cells, respectively, compared to the control condition (Control: -39.6 ± 0.5 mV, $n = 65$; NALCN+: -27.9 ± 1.2 mV, $n = 96$, $P < .0001$; NALCN-: -44.9 ± 1.1 mV, $n = 44$, $P < .001$; Figure 3B). As expected, the most depolarized NALCN+ GH₃ cells correspond to the electrically silent ones (Figure S3). However, there was not any significant difference in the RMP between

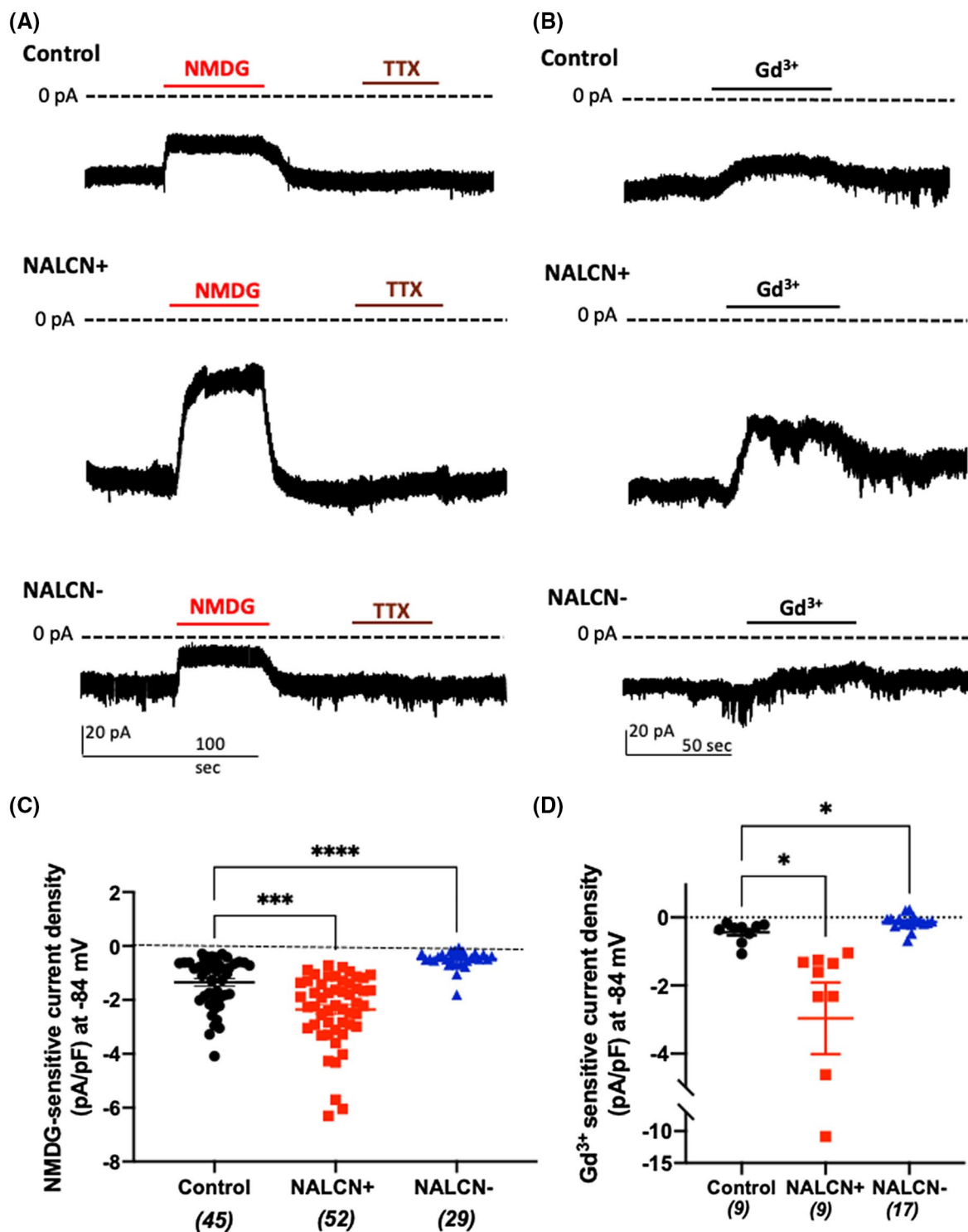


FIGURE 4 NALCN mediates a TTX-resistant and Gd^{3+} -sensitive sodium background conductance. A, Representative traces obtained on cells held at -84 mV (HP) during application/wash of an extracellular Na^+ -free solution (replaced with NMDG) followed by an application/wash of TTX for a control GH₃ cell (top), a NALCN overexpressing GH₃ cell (NALCN+, middle), and a knockdown GH₃ cell (NALCN–, bottom). Red and purple bars (above each recording) indicate when extracellular Na^+ was replaced with NMDG and when TTX ($1 \mu\text{mol/L}$) was applied, respectively. B, Representative traces obtained on cells held at -84 mV (HP) during application of Gd^{3+} for a control GH₃ cell (top), a NALCN overexpressing GH₃ cell (NALCN+, middle), and a knockdown GH₃ cell (NALCN–, bottom). Black bars (above each recording) indicate when Gd^{3+} ($200 \mu\text{mol/L}$) was applied. C, Density of the external Na^+ -dependent background current (Na^+ -free) for Control GH₃ cells (-1.3 ± 0.1 pA/pF, $n = 45$), NALCN+ GH₃ cells (-2.3 ± 0.1 pA/pF, $n = 52$) and NALCN– GH₃ cells (NALCN–: -0.4 ± 0.06 pA/pF, $n = 29$). Statistical analysis: Kruskal-Wallis with FDR corrected post hoc tests; *** $P < .001$, **** $P < .0001$ compared to Control. The Na^+ background current density was deduced after subtracting the current trace during NMDG application from the control current. D, Density of the Gd^{3+} -sensitive current for Control GH₃ cells (-0.4 ± 0.1 pA/pF, $n = 9$), NALCN+ GH₃ cells (-2.9 ± 1 pA/pF, $n = 9$) and NALCN– GH₃ cells (-0.1 ± 0.05 pA/pF, $n = 17$). Statistical analysis: Kruskal-Wallis with FDR corrected post hoc tests; * $P < .05$ compared to Control. The Gd^{3+} -sensitive background current density was deduced after subtracting the current trace during Gd^{3+} application from the control current

silent and spiking cells in the NALCN– condition (Figure S3). A significant and reversible hyperpolarization of the RMP was also observed with the three GH₃ cells groups when extracellular Na^+ was substituted with NMDG (Control: -41.2 ± 0.8 mV vs -44.4 ± 0.7 mV, $n = 25$, $P < .0001$; NALCN+: -26.6 ± 1.7 mV vs -35.7 ± 1.5 mV, $n = 57$, $P < .0001$; NALCN–: -45.4 ± 0.8 mV vs -48.8 ± 1.3 mV, $n = 22$, $P < .01$; Figure 3A,C). A further analysis showed a significant increase of the ΔRMP (ie, RMP with extracellular Na^+ minus RMP in Na^+ -free condition) when NALCN was overexpressed compared of the control condition (Control: -2.5 ± 0.6 mV, $n = 25$; NALCN+: -9 ± 0.9 mV, $n = 57$, $P < .0001$; Figure 3C). However, the ΔRMP was not significantly changed when NALCN was knocked down compared to the control condition (NALCN–: -3.4 ± 1.1 mV, $n = 22$, $P = .7$). Nonetheless, our results demonstrated that NALCN contributed to the RMP of GH₃ cells.

3.4 | NALCN mediates a TTX-resistant and Gd^{3+} -sensitive sodium background conductance

We next switched to a voltage-clamp mode to determine a contribution of NALCN in a Na^+ background conductance in GH₃ cells (Figure 4). We first performed experiments to examine the holding current and the effect of external Na^+ removal (ie, NMDG-substituted) when cells were held at -84 mV. Indeed, this value corresponds to the calculated equilibrium potential for K^+ ions in our experimental conditions thus preventing any contamination by K^+ current from occurring (Figure 4A). The holding current density was found to be significantly different in the three conditions. Indeed, it was found to be higher and lower in NALCN+ and NALCN– GH₃ cells, respectively, compared to the control condition (Control: -2.1 ± 0.2 pA/pF, $n = 45$; NALCN+: -3.4 ± 0.2 pA/pF, $n = 52$, $P < .0001$; NALCN–: -0.7 ± 0.05 pA/pF, $n = 29$, $P < .001$; Figure S4A). Furthermore, replacing external Na^+ with the impermeant cation NMDG in the three

GH₃ cell lines resulted in a significant decrease of the holding current in cells. Importantly, NMDG application revealed that this holding current carried by Na^+ ions, designated by Na^+ background current, was significantly larger (~ 1.7 -fold increase) in cells overexpressing human NALCN compared to the control group (Control: -1.3 ± 0.1 pA/pF, $n = 45$; NALCN+: -2.3 ± 0.1 pA/pF, $n = 52$, $P < .0001$; Figure 4C). Conversely, the Na^+ background current was significantly smaller (~ 2.8 -fold decrease) in the knockdown condition compared to the control group (NALCN–: -0.5 ± 0.06 pA/pF, $n = 29$, $P < .001$). These results showed that the expression level of NALCN in GH₃ cells impacts the Na^+ background conductance. This Na^+ background conductance was not inhibited by TTX ($1 \mu\text{mol/L}$; Figure 4A, Figure S4B). Indeed, we observed that TTX slightly increased the holding current in some cells. We next examined the sensitivity of the current to Gd^{3+} ($200 \mu\text{mol/L}$; Figure 4B). We found that Gd^{3+} significantly reduced the holding current density of the background conductance in the three conditions (Figure 4D). This reduction was significantly higher in the NALCN+ condition but was significantly lower in the NALCN– condition compared to the control group (Control: -0.4 ± 0.1 pA/pF, $n = 9$; NALCN+: -2.9 ± 1 pA/pF, $n = 9$, $P = .02$; NALCN–: -0.1 ± 0.05 pA/pF, $n = 17$, $P = .02$). Taken together, our data showed that NALCN behaves as a TTX-resistant and Gd^{3+} -sensitive Na^+ leak channel in GH₃ cells.

3.5 | The Na^+ background conductance exhibits a linear current-voltage relationship in GH₃ cells

The current-voltage relationship of the Na^+ background conductance was examined for membrane potentials ranging from -100 to -30 mV in both control and NALCN+ GH₃ cell lines (Figure 5). To do so, we used a voltage step protocol on cells held at -30 mV in the presence and the absence of extracellular Na^+ (Figure 5A). The subtracted current reflecting the Na^+ -dependent background conductance

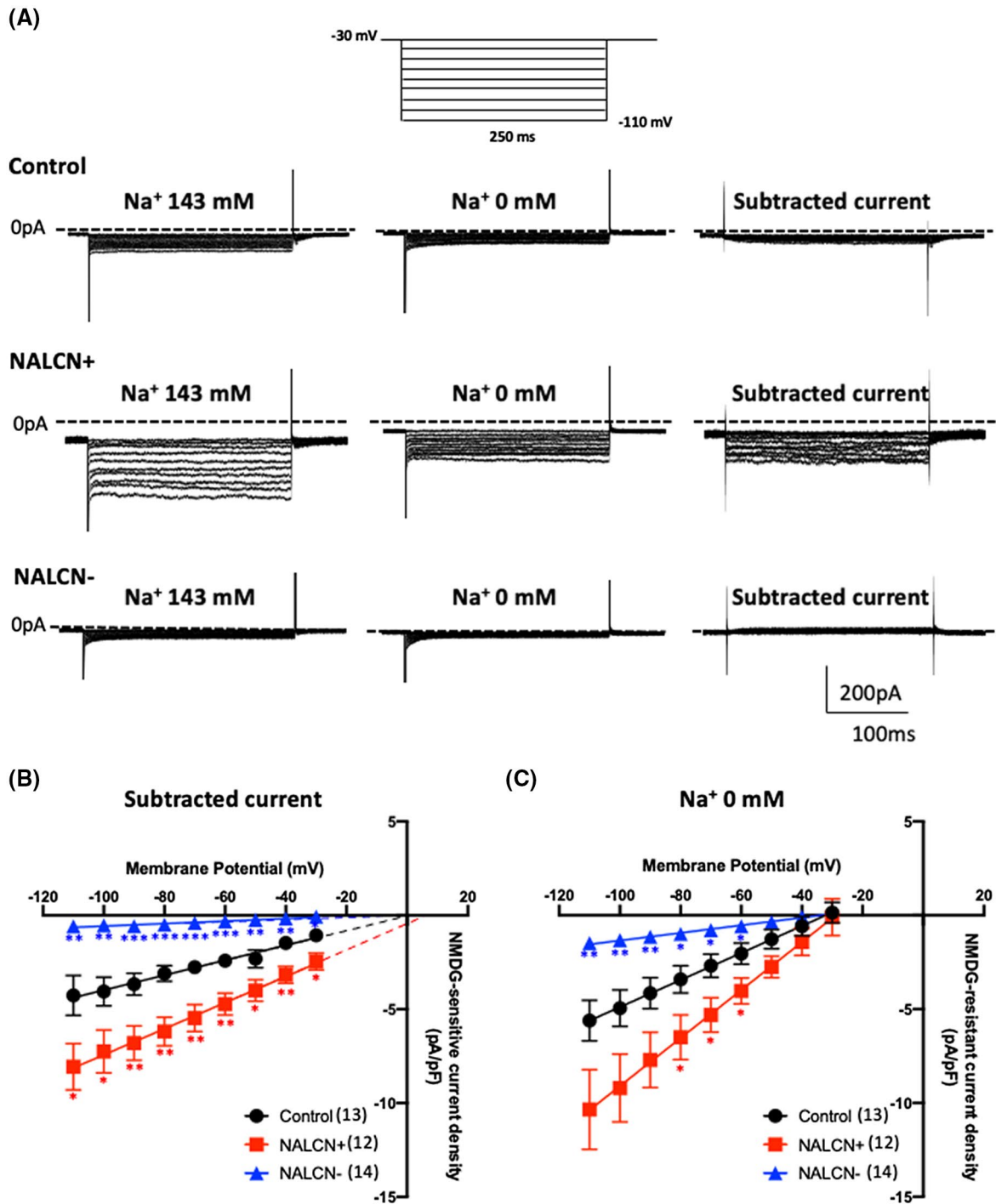


FIGURE 5 The sodium background conductance exhibits a linear current-voltage relationship in GH₃ cells. A, Representative current traces elicited by a membrane voltage step protocol (test pulses of 250 ms from -30 to -110 mV with 10 mV decrements) with cells held at -30 mV, in the presence and absence of extracellular Na⁺ for a control GH₃ cell (top), a NALCN+ GH₃ cell (middle), and a NALCN- GH₃ cell (bottom). Traces were subtracted to isolate the Na⁺-dependent component of the NALCN current for both control and NALCN+ GH₃ cells. B, Current-voltage relationship for the Na⁺ background current in Control (n = 13), NALCN+ (n = 12) and NALCN- (n = 14) GH₃ cells. A linear regression analysis indicated an extrapolated reversal potential E_{rev} of +0.12, +7.05 and -13 mV in control, NALCN+, and NALCN- GH₃ cells, respectively. The mean slope conductance value of 39.8 ± 7.2 pS/pF, 69.4 ± 10.1 pS/pF and 6.7 ± 1.5 pS/pF, in Control, NALCN+, and NALCN- GH₃ cells, respectively, was deduced from individual linear regression analyses for each cell. C, Current-voltage relationship for the NMDG-resistant current in Control (n = 13), NALCN+ (n = 12) and NALCN- (n = 14) GH₃ cells. A linear regression analysis indicated an extrapolated reversal potential E_{rev} of -32.09 mV, -28.82 and -33.65 mV in control, NALCN+, and NALCN- GH₃ cells, respectively. The mean slope conductance value of 72.1 ± 9.2 pS/pF, 129.7 ± 15.9 pS/pF and 20.3 ± 2.4 pS/pF, in Control, NALCN+, and NALCN- GH₃ cells, respectively, was deduced from individual linear regression analyses for each cell. Statistical analysis for both (B and C): two-ways ANOVA with *Cell types* as between subjects' factor and *Time* as within subjects, repeated measures factor; FDR corrected post hoc tests; * P < .05, ** P < .01, *** P < .001, compared to Control

was then used to determine its current-voltage relationship (Figure 5B). We found a linear current-voltage relationship within the range of -110 to -30 mV with an extrapolated reversal potential E_{rev} of $+0.1$, $+7.1$ and -13 mV in Control, NALCN+, and NALCN- GH_3 cells, respectively (Figure 5B). The corresponding slope conductance of this NMDG-sensitive current was 39.8 ± 7.2 pS/pF, 69.4 ± 10.1

pS/pF and 6.7 ± 1.5 pS/pF, in Control, NALCN+, and NALCN- GH_3 cells, respectively. Compared to the Control condition, current densities were found to be significantly lower in the NALCN- condition and significantly higher in the NALCN+ condition at all tested potentials. These results are consistent with a linear (ohmic) Na^+ -dependent background conductance as previously described in this cell type⁶

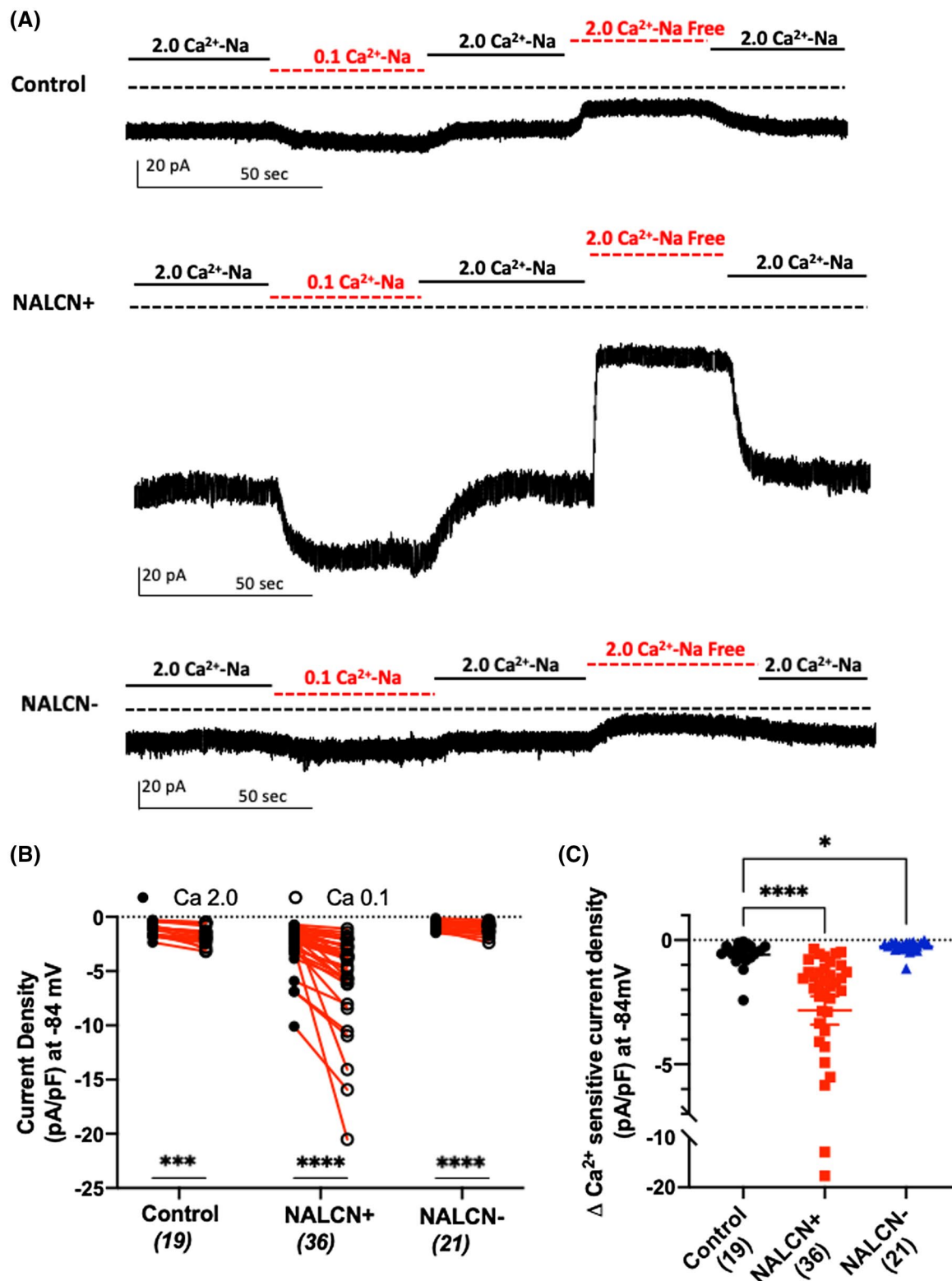


FIGURE 6 The NALCN current is regulated by extracellular Ca^{2+} in GH_3 cells. A, Representative traces obtained on cells held at -84 mV (HP) during successive application/wash of an extracellular low Ca^{2+} solution (ie, 0.1 mmol/L) and an extracellular Na^+ -free solution (replaced with NMDG) for a control GH_3 cell (top), a NALCN-overexpressing GH_3 cell (NALCN+, middle) and a NALCN-knocked-down GH_3 cell (NALCN-, bottom). B, Increase of the background conductance when lowering the Ca^{2+} concentration from 2 to 0.1 mmol/L (Control: 1.04 ± 0.1 pA/pF vs 1.6 ± 0.2 pA/pF, $n = 19$; NALCN+: 2.5 ± 0.3 pA/pF vs 5.3 ± 0.7 pA/pF, $n = 36$; NALCN-: 0.7 ± 0.1 pA/pF vs 1 ± 0.1 pA/pF, $n = 21$). Statistical analysis: for each cell type, paired t test; *** $P < .001$, **** $P < .0001$, compared to Ca^{2+} 2 mmol/L. The Na^+ background current density in extracellular Ca^{2+} 2 and 0.1 mmol/L was obtained by subtracting the current trace during NMDG application from the control current at the considered extracellular Ca^{2+} concentration. C, $\Delta I_{\text{Ca}^{2+}\text{-sensitive}}$ (ie, $I_{\text{NMDG-sensitive}}$ with extracellular Ca^{2+} 0.1 mmol/L minus $I_{\text{NMDG-sensitive}}$ with extracellular Ca^{2+} 2 mmol/L) when NALCN was overexpressed compared to the control condition (Control: -0.6 ± 0.1 pA/pF, $n = 19$; NALCN+: -2.8 ± 0.6 pA/pF, $n = 36$; NALCN-: -0.2 ± 0.05 pA/pF, $n = 21$). Statistical analysis: Kruskal-Wallis with FDR corrected post hoc tests; * $P < .05$, **** $P < .0001$ compared to Control

in every condition, Control, NALCN+, and NALCN- cell lines, suggesting that the Na^+ -dependent background in GH_3 cell line is mainly carried out by NALCN channel. However, in the low external Na^+ (NMDG-substituted) condition a, leak current was still observed in the Control and NALCN+ conditions (Figure 5A,C), with a slope conductance value of 72.1 ± 9.2 pS/pF, 129.7 ± 15.9 pS/pF, and 20.3 ± 2.4 pS/pF, in Control, NALCN+, and NALCN- GH_3 cells, respectively, for this NMDG-resistant current. This NMDG-resistant leak current was significantly reduced in the NALCN- condition within the -110 to -50 mV range and conversely, significantly increased in the NALCN+ condition within the -80 to -60 mV range. This suggests that NALCN is not a pure Na^+ channel in GH_3 cells and might conduct other ions such as K^+ and Ca^{2+} as previously suggested.¹⁷ Additional experiments will be required in the future to investigate with greater detail the permeation properties of NALCN in GH_3 cells.

3.6 | The NALCN current is regulated by extracellular Ca^{2+} in GH_3 cells

An important feature of NALCN is its negative regulation by extracellular Ca^{2+} in native neurons as well as when it is heterologously expressed in cell lines such as the HEK-293T and neuronal NG108-15 cell lines.^{18,34-38} Indeed, these studies have shown that switching from a Ca^{2+} concentration of 2 to 0.1 mmol/L resulted in a significant increase in the current amplitude generated by NALCN. Thus, we checked whether this property could be conserved in our pituitary cell model (Figure 6). Using voltage-clamp recordings at a holding potential of -84 mV, we found that a decrease of the Ca^{2+} concentration from 2 to 0.1 mmol/L resulted in a significant increase in the background conductance in the three conditions, Control, NALCN+, and NALCN- GH_3 cells (Control: -1.04 ± 0.1 pA/pF vs -1.6 ± 0.2 pA/pF, $n = 19$, $P < .001$; NALCN+: -2.5 ± 0.3 pA/pF vs -5.3 ± 0.7 pA/pF, $n = 36$, $P < .0001$; NALCN-: -0.7 ± 0.07 pA/pF vs -1 ± 0.1 pA/pF, $n = 21$, $P < .0001$; Figure 6A,B). A further analysis showed a significant increase of the $\Delta I_{\text{Ca}^{2+}\text{-sensitive}}$ (ie, $I_{\text{NMDG-sensitive}}$ with extracellular Ca^{2+} 0.1 mmol/L minus $I_{\text{NMDG-sensitive}}$ with

extracellular Ca^{2+} 2 mmol/L) when NALCN was heterologously expressed compared to the control condition (Control: -0.6 ± 0.1 pA/pF, $n = 19$; NALCN+: -2.8 ± 0.6 pA/pF, $n = 36$, $P < .0001$; Figure 6C). Conversely, the $\Delta I_{\text{Ca}^{2+}\text{-sensitive}}$ was reduced in NALCN- GH_3 cells (-0.2 ± 0.05 pA/pF, $n = 21$, $P = .04$; Figure 6C). Our results demonstrated that NALCN is negatively modulated by extracellular Ca^{2+} in GH_3 cells.

3.7 | Extracellular Ca^{2+} modulates both electrical activity and the RMP in GH_3 cells

We next examined how extracellular Ca^{2+} could modulate the RMP of GH_3 cells through NALCN (Figure 7). Indeed, a regulation of the RMP by extracellular Ca^{2+} was previously described in lactotrophs, somatotrophs as well as in the pituitary GC cell line.⁷⁻⁹ As expected, since voltage-gated Ca^{2+} channels are involved in GH_3 action potentials,^{32,39} reducing extracellular Ca^{2+} from 2 to 0.1 mmol/L prevented action potential firing in all conditions (Figure 7A). Importantly, our data revealed a marked and reversible depolarization of the V_m of GH_3 cells when extracellular Ca^{2+} was reduced in the three conditions (Control: -39 ± 0.9 vs -26.6 ± 1.4 mV, $n = 26$, $P < .0001$; NALCN+: -33.4 ± 1.4 vs -17 ± 1.3 mV, $n = 30$, $P < .0001$; NALCN-: -45.1 ± 1 vs -32.6 ± 1.9 mV, $n = 15$, $P < .0001$; Figure 7A,B). A further analysis showed a significant increase of the ΔV_m (ie, V_m with extracellular Ca^{2+} at 2 mmol/L minus V_m with extracellular Ca^{2+} at 0.1 mmol/L) when NALCN was overexpressed compared to the Control condition (Control: -12.4 ± 1 mV, $n = 26$; NALCN+: -17.4 ± 0.8 mV, $n = 30$, $P = .0015$; Figure 7C). In addition, the time to reach half-maximum depolarization following extracellular Ca^{2+} decrease was \sim twofold reduced when NALCN was overexpressed, compared to the Control condition (Control: 11.8 ± 0.7 seconds, $n = 26$; NALCN+: 5.6 ± 0.6 seconds, $n = 30$, $P < .001$; Figure 7D). However, in the NALCN- condition, there was not any significant difference compared to the Control condition for both the ΔV_m (NALCN-: -12.5 ± 1.3 mV, $n = 15$, $P = .99$) and the time to reach half-maximum depolarization (NALCN-:

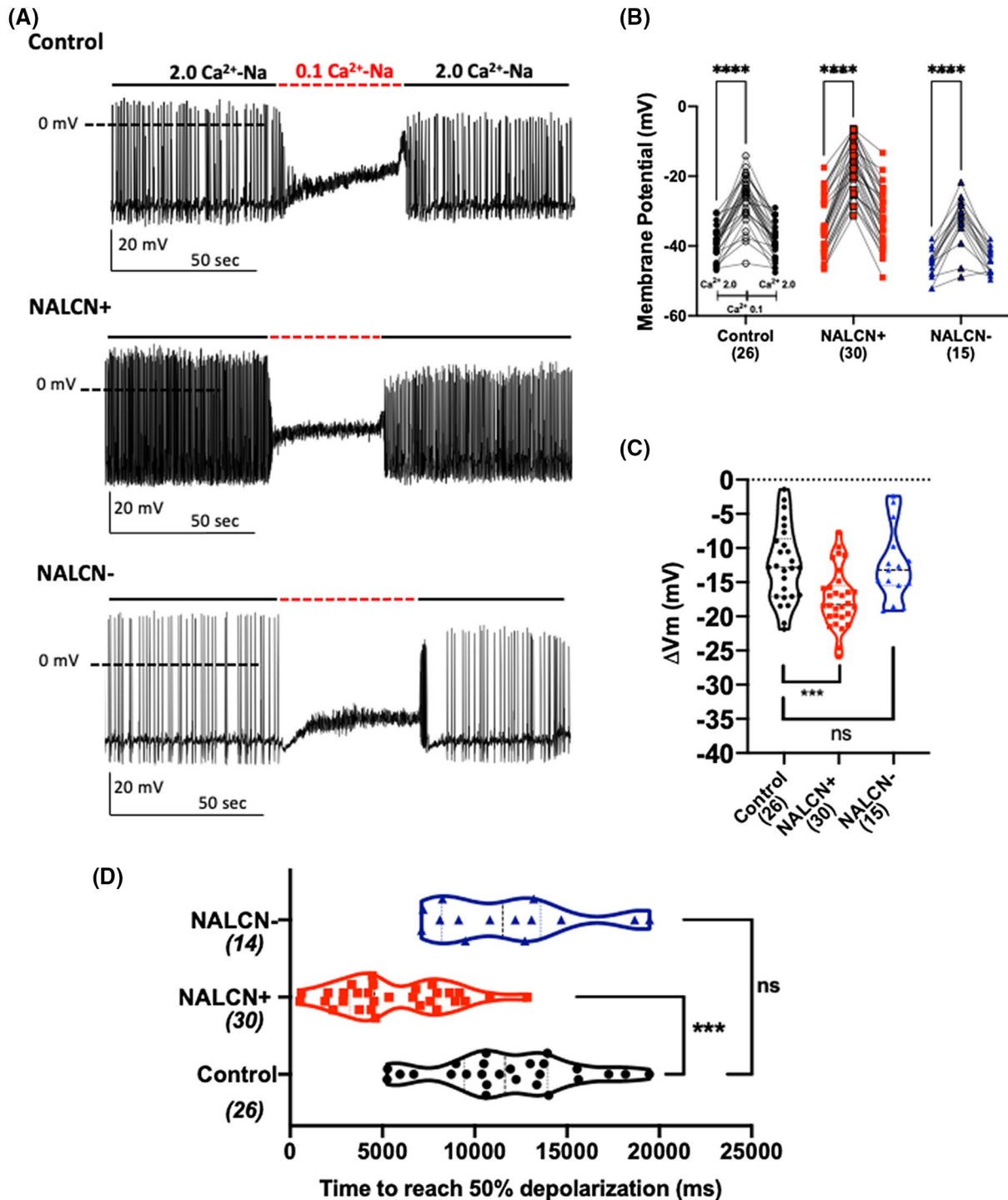


FIGURE 7 Extracellular Ca^{2+} modulates both electrical activity and RMP in GH₃ cells. A, Representative traces of membrane potential recordings for the control, NALCN+, and NALCN- conditions. Extracellular Ca^{2+} was transiently switched from 2 to 0.1 mmol/L (see the red dashed bars above each recording for duration). B, Summary of the RMP change when Ca^{2+} was switched from 2 to 0.1 mmol/L (Control: -39 ± 0.9 mV vs -26.6 ± 1.4 mV, $n = 26$; NALCN+: -33.4 ± 1.4 mV vs -17 ± 1.3 mV, $n = 30$; NALCN-: -45.1 ± 1 mV vs -32.6 ± 1.9 mV, $n = 15$). Statistical analysis: for each cell type, paired t test; **** $P < .0001$, compared to Ca^{2+} 2 mmol/L. C, ΔRMP (ie, RMP with extracellular Ca^{2+} at 2 mmol/L minus RMP with extracellular Ca^{2+} at 0.1 mmol/L) when NALCN is overexpressed or knocked down compared of the control condition (Control: -12.4 ± 1 mV, $n = 26$; NALCN+: -17.4 ± 0.8 mV, $n = 30$; NALCN-: -12.5 ± 1.3 mV, $n = 15$). Statistical analysis: One-way ANOVA with FDR corrected post hoc tests; *** $P < .001$ compared to Control. D, Half-time to reach the plateau phase of the RMP following extracellular Ca^{2+} decrease (Control: 11.8 ± 0.7 sec, $n = 26$; NALCN+: 5.6 ± 0.6 sec, $n = 30$; NALCN-: 13 ± 1.6 sec, $n = 15$). Statistical analysis: One-way ANOVA with FDR corrected post hoc tests; *** $P < .001$ compared to Control. This value was calculated as the time to reach 50% of the maximum depolarization following application of an extracellular solution with Ca^{2+} 0.1 mmol/L.

13 ± 1.6 seconds, $n = 15$, $P = .5$). These data suggested that, although NALCN can contribute to the regulation of the Vm by extracellular Ca^{2+} , its contribution is too low in GH₃ cells to be sufficient to play a major role in this process.

3.8 | NALCN regulates prolactin secretion of GH₃ cells

Somatolactotroph GH₃ cells spontaneously secrete both Growth Hormone (GH) and Prolactin (PRL).^{40,41} This secretion depends on the electrical activity and is positively modulated by application of Thyrotropin releasing hormone (TRH).^{1,42,43} Since NALCN regulates excitability of GH₃ cells, we hypothesized its knockdown could impair hormone release. To address this point, we measured both basal and TRH-stimulated PRL secretion in the culture medium using an Enzyme Immunometric Assay (see the Materials and Methods section; Figure 8). We found that basal PRL secretion was significantly reduced (~1.7- to 2-fold) in the NALCN⁻ condition compared to the Control condition at all tested times of incubation (5 minutes: Control, 4.7 ± 0.58 ng/mg, NALCN⁻, 2.3 ± 0.23 ng/mg, $N = 3$, $P = .01$; 15 minutes: Control, 6.55 ± 0.6 ng/mg, NALCN⁻, 3.7 ± 0.5 ng/mg, $N = 3$, $P = .004$; 60 minutes: Control, 12.16 ± 1.1 ng/mg, NALCN⁻, 6.97 ± 0.85 ng/mg, $N = 3$, $P < .0001$; Figure 8). As expected, TRH (100 nmol/L) significantly increased (~1.4 to 1.8-fold) PRL release in Control GH₃ cells when measured at 15 and 60 minutes, but not at 5 minutes, following application (5 minutes: 6 ± 0.74 ng/mg, $N = 3$, $P = .08$; 15 minutes: 9.52 ± 0.8 ng/mg, $N = 3$, $P = .003$; 60 minutes: 21.22 ± 1.3 ng/mg, $N = 3$, $P < .0001$). The TRH-stimulated PRL secretion was significantly reduced (~2.2- to 2.9-fold) in the NALCN⁻ condition (5 minutes: 2.65 ± 0.3 ng/mg, $N = 3$, $P = .0019$; 15 minutes: 3.62 ± 0.15 ng/mg, $N = 3$, $P < .0001$; 60 minutes: 7.44 ± 0.61 ng/mg, $N = 3$, $P < .0001$). PRL secretion was not even significantly different from the NALCN⁻ condition without TRH application (5 minutes: $N = 3$, $P = .2$; 15 minutes: $N = 3$, $P = .2$; 60 minutes: $N = 3$, $P = .2$). Taken together, these results demonstrated that subsequently to its regulation of cell excitability, NALCN contributes to both basal and stimulated PRL secretion of GH₃ cells.

4 | DISCUSSION

4.1 | A role of NALCN in pituitary endocrine cell excitability

The data presented in this study demonstrate that the sodium leak channel NALCN as well as its ancillary subunits are endogenously expressed in GH₃ cells at least at the mRNA level. We show that in this pituitary cell line, NALCN conducts a

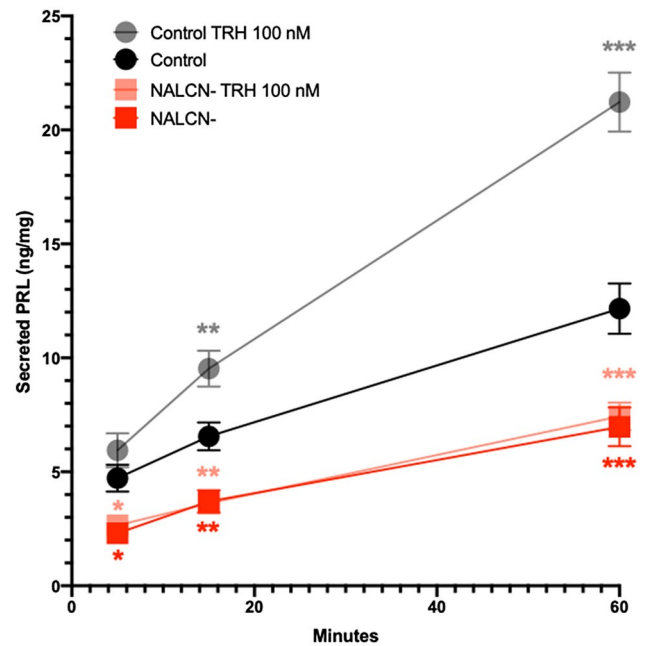


FIGURE 8 NALCN regulates prolactin secretion of GH₃ cells. The involvement of NALCN in prolactin (PRL) secretion was determined in both basal and Thyrotropin releasing hormone (TRH)-stimulated conditions using an Enzyme Immunometric Assay. Results are presented as ng of hormone released per mg of cellular protein \pm SEM. Basal level of secreted PRL was found to be significantly decreased in the NALCN⁻ condition compared to the Control condition (5 min: Control, 4.7 ± 0.58 ng/mg, NALCN⁻, 2.3 ± 0.23 ng/mg, $N = 3$; 15 min: Control, 6.55 ± 0.6 ng/mg, NALCN⁻, 3.7 ± 0.5 ng/mg, $N = 3$; 60 min: Control, 12.16 ± 1.1 ng/mg, NALCN⁻, 6.97 ± 0.85 ng/mg, $N = 3$). Application of TRH significantly increased PRL release in Control GH₃ cells when measured at 15 min and 60 min (5 min: 6 ± 0.74 ng/mg, $N = 3$; 15 min: 9.52 ± 0.8 ng/mg, $N = 3$; 60 min: 21.22 ± 1.3 ng/mg, $N = 3$). The TRH-induced increase in PRL secretion was significantly reduced in the NALCN⁻ condition (5 min: 2.65 ± 0.3 ng/mg, $N = 3$; 15 min: 3.62 ± 0.15 ng/mg, $N = 3$; 60 min: 7.44 ± 0.61 ng/mg, $N = 3$). Statistical analysis: three-ways ANOVA with *Cell types* and *Treatment* (ie, TRH) as between subjects' factors and *Time* as within subjects repeated measures factor; FDR corrected post hoc tests; * $P < .05$, ** $P < .01$, *** $P < .001$ compared to Control

Na^+ background current, which regulates the RMP and the electrical activity of GH₃ cells. Our findings are in good agreement with the described properties and cellular roles of NALCN in neurons.¹⁷⁻²⁶ In addition to the central nervous system, the NALCN-encoding mRNA was also detected in heart and endocrine tissues, including the pituitary gland.^{28,44} Importantly, a Na^+ background conductance was described in several cell types of the anterior pituitary gland, including in the somatolactotroph GH₃ cell line.⁶⁻¹⁵ An important finding of this study is that the excitability properties of GH₃ cells rely on the expression level of NALCN. We report that the overexpression of NALCN depolarized the RMP while its knockdown led to a more negative RMP of GH₃ cells.

Also, considering the electrically active GH₃ cells in each condition, the firing frequency was increased in GH₃ cells overexpressing NALCN and decreased in GH₃ cells knocked down for NALCN. Overall, our study points to the role of NALCN as an important player of the cellular excitability in the anterior pituitary cellular model, GH₃. However, we noticed that the Δ RMP values (ie, RMP with extracellular Na⁺ minus RMP without extracellular Na⁺) were not significantly different between the NALCN[−] and Control GH₃ cells. It may be that the endogenous NALCN current is not fully inhibited by the knockdown strategy employed here and/or that some changes in GH₃ intrinsic electrophysiological properties may not appear as significant by removing extracellular Na⁺. The discovery of selective NALCN blockers would be of great help in the future to better decipher the cellular role(s) of NALCN.

4.2 | The properties of the Na⁺ background current in GH₃ cells matches those of NALCN

Using a RNA interference-based approach to knockdown NALCN expression in GH₃ cells, we observed a significant reduction of the current density of the Na⁺ background conductance (external Na⁺ substituted by NMDG), revealing that a large fraction of this Na⁺ background conductance was carried out by NALCN. Conversely, overexpression of the human NALCN resulted in a significantly larger current density of the Na⁺ background conductance, validating further the ability of GH₃ cells to functionally express NALCN channel. This NALCN-related Na⁺ background conductance was blocked by Gd³⁺ and insensitive to TTX. Importantly, we describe here that the NALCN-related Na⁺ background current in GH₃ cells was significantly increased when extracellular Ca²⁺ was reduced from 2 to 0.1 mmol/L. This is also a key feature of NALCN, which is negatively regulated by extracellular Ca²⁺.^{18,34–38} However, although reducing Ca²⁺ was seen to modulate NALCN+ cell excitability (Figure 7), no significant change could be seen between NALCN[−] and Control conditions suggesting that Ca²⁺ regulation of endogenous NALCN channel may be limited –or yet to be identified– in native GH₃ cells. Using a RNA interference approach to knockdown NALCN expression, a residual Na⁺ background conductance in GH₃ cells was still present. Considering that RNA interference has an ~80% efficiency at the mRNA level, the remaining Na⁺ background current could result from a residual expression of NALCN. This remaining Na⁺ background current could also reflect a contribution of other ion channels as Gd³⁺ application had a smaller effect than Na⁺ removal on Control (-1.3 ± 0.1 when Na⁺ was removed vs -0.4 ± 0.1 pA/pF when Gd³⁺ was applied) and NALCN[−] GH₃ cells (-0.5 ± 0.06 vs -0.1 ± 0.05 pA/pF; Figure 4) but a similar or even larger effect than

Na⁺ removal in NALCN+ GH₃ cells (-2.3 ± 0.1 pA/pF vs -2.9 ± 1 pA/pF). Indeed, several studies also suggested that TRP channels could be involved in the Na⁺ background conductance of anterior pituitary cells as well as GH₃ cells.^{11,12,15} This hypothesis was based on detectable mRNA expression of some TRP channels in these cell types. However, no genetic manipulation was carried out with any TRP channel. TRP channels were also suggested following the use of some more or less specific pharmacological compounds. For example, 2-APB (100 μ mol/L) was used as a TRPC inhibitor to show that this channel sub-family is involved in the Na⁺ background conductance of rat pituitary cells.¹² However, a recent study revealed that NALCN current may be blocked by 2-APB with a ~50% potency at the same concentration.⁴⁵ Similarly, other compounds such as SKF96365 or flufenamic acid may also affect NALCN activity at the used concentration. Nevertheless, the NALCN current appears to represent a large fraction of the Na⁺ background current in GH₃ cells and to play a role in regulating the RMP and excitability in these cells. We also observed an unexpected increase and decrease of a Na⁺-independent current following NALCN overexpression and knockdown, respectively (Figure 5A,C). One may hypothesize this Na⁺-independent component may result from the permeation of other ions through NALCN. Alternatively, one may speculate that a change in the expression level/activity of NALCN could modify the expression/function of other channels either directly through allosteric modulation or indirectly by modifying intracellular Ca²⁺ signaling and subsequently gene transcription. Additional experiments are now required to clarify the origin of this Na⁺-independent current.

4.3 | Toward the physiological role(s) of NALCN in pituitary cells

Using GH₃ cells in which the expression level of NALCN is monitored (knockdown, overexpression), our findings revealed that NALCN could play a significant role in pituitary cells. Although the physiological relevance of these findings remains to be determined in native pituitary cells, we can hypothesize that the physiology of this endocrine tissue, its excitability and hormone secretion properties, would rely on the level of NALCN activity. In keeping with this idea, we demonstrated a role for NALCN in both basal and TRH-induced PRL secretion in GH₃ cells. This role in hormone secretion is in agreement with studies showing that replacing extracellular Na⁺ by choline reduce basal PRL secretion from rat primary lactotrophs.^{7,11,46} However, a role of extracellular Na⁺ on TRH-induced PRL secretion from primary cells was not clearly demonstrated.⁴⁶ Our findings can be modeled as follow: a reduced level of NALCN activity leads to hyperpolarization and reduced excitability and conversely,

8. Kwiecien R, Robert C, Cannon R, et al. Endogenous pacemaker activity of rat tumour somatotrophs. *J Physiol.* 1998;508(Pt 3):883-905.
9. Tsaneva-Atanasova K, Sherman A, van Goor F, Stojilkovic SS. Mechanism of spontaneous and receptor-controlled electrical activity in pituitary somatotrophs: experiments and theory. *J Neurophysiol.* 2007;98:131-144.
10. Kucka M, Kretschmannova K, Murano T, et al. Dependence of multidrug resistance protein-mediated cyclic nucleotide efflux on the background sodium conductance. *Mol Pharmacol.* 2010;77:270-279.
11. Kucka M, Kretschmannova K, Stojilkovic SS, Zemkova H, Tomic M. Dependence of spontaneous electrical activity and basal prolactin release on nonselective cation channels in pituitary lactotrophs. *Physiol Res.* 2012;61:267-275.
12. Tomic M, Kucka M, Kretschmannova K, et al. Role of nonselective cation channels in spontaneous and protein kinase A-stimulated calcium signaling in pituitary cells. *Am J Physiol Endocrinol Metab.* 2011;301:E370-379.
13. Liang Z, Chen L, McClafferty H, et al. Control of hypothalamic-pituitary-adrenal stress axis activity by the intermediate conductance calcium-activated potassium channel, SK4. *J Physiol.* 2011;589:5965-5986.
14. Zemkova H, Tomic M, Kucka M, Aguilera G, Stojilkovic SS. Spontaneous and CRH-induced excitability and calcium signaling in mice corticotrophs involves sodium, calcium, and cation-conducting channels. *Endocrinology.* 2016;157:1576-1589.
15. Kayano T, Sasaki Y, Kitamura N, et al. Persistent Na(+) influx drives L-type channel resting Ca(2+) entry in rat melanotrophs. *Cell Calcium.* 2019;79:11-19.
16. Snutch TP, Monteil A. The sodium "leak" has finally been plugged. *Neuron.* 2007;54:505-507.
17. Lu B, Su Y, Das S, Liu J, Xia J, Ren D. The neuronal channel NALCN contributes resting sodium permeability and is required for normal respiratory rhythm. *Cell.* 2007;129:371-383.
18. Lu TZ, Feng ZP. A sodium leak current regulates pacemaker activity of adult central pattern generator neurons in *Lymnaea stagnalis*. *PLoS One.* 2011;6:e18745.
19. Xie L, Gao S, Alcaire SM, et al. NLF-1 delivers a sodium leak channel to regulate neuronal excitability and modulate rhythmic locomotion. *Neuron.* 2013;77:1069-1082.
20. Gao S, Xie L, Kawano T, et al. The NCA sodium leak channel is required for persistent motor circuit activity that sustains locomotion. *Nat Commun.* 2015;6:6323.
21. Flourakis M, Kula-Eversole E, Hutchison AL, et al. A conserved bicycle model for circadian clock control of membrane excitability. *Cell.* 2015;162:836-848.
22. Lutas A, Lahmann C, Soumillon M, Yellen G. The leak channel NALCN controls tonic firing and glycolytic sensitivity of substantia nigra pars reticulata neurons. *Elife.* 2016;5:15271.
23. Shi Y, Abe C, Holloway BB, et al. Nalc is a "Leak" sodium channel that regulates excitability of brainstem chemosensory neurons and breathing. *J Neurosci.* 2016;36:8174-8187.
24. Yeh SY, Huang WH, Wang W, et al. Respiratory network stability and modulatory response to substance P require nalcn. *Neuron.* 2017;94(294-303):e294.
25. Ford NC, Ren D, Baccetti ML. NALCN channels enhance the intrinsic excitability of spinal projection neurons. *Pain.* 2018;159:1719-1730.
26. Funato H, Miyoshi C, Fujiyama T, et al. Forward-genetics analysis of sleep in randomly mutagenized mice. *Nature.* 2016;539:378-383.
27. Cochet-Bissuel M, Lory P, Monteil A. The sodium leak channel, NALCN, in health and disease. *Front Cell Neurosci.* 2014;8:132.
28. Swayne LA, Mezghrani A, Varrault A, et al. The NALCN ion channel is activated by M3 muscarinic receptors in a pancreatic beta-cell line. *EMBO Rep.* 2009;10:873-880.
29. Barde I, Salmon P, Trono D. (2010) Production and titration of lentiviral vectors. *Curr Protoc Neurosci.* Chapter 4, Unit 4 21.
30. Untergasser A, Cutcutache I, Koressaar T, et al. Primer3—new capabilities and interfaces. *Nucleic Acids Res.* 2012;40:e115.
31. Pfaffl MW. A new mathematical model for relative quantification in real-time RT-PCR. *Nucleic Acids Res.* 2001;29:e45.
32. Kidokoro Y. Spontaneous calcium action potentials in a clonal pituitary cell line and their relationship to prolactin secretion. *Nature.* 1975;258:741-742.
33. Taraskevich PS, Douglas WW. Electrical behaviour in a line of anterior pituitary cells (GH cells) and the influence of the hypothalamic peptide, thyrotrophin releasing factor. *Neuroscience.* 1980;5:421-431.
34. Lu B, Zhang Q, Wang H, Wang Y, Nakayama M, Ren D. Extracellular calcium controls background current and neuronal excitability via an UNC79-UNC80-NALCN cation channel complex. *Neuron.* 2010;68:488-499.
35. Philippart F, Khaliq ZM. Gi/o protein-coupled receptors in dopamine neurons inhibit the sodium leak channel NALCN. *Elife.* 2018;7:40984.
36. Bouasse M, Impheng H, Servant Z, Lory P, Monteil A. Functional expression of CLIFAHDD and IHPRF pathogenic variants of the NALCN channel in neuronal cells reveals both gain- and loss-of-function properties. *Sci Rep.* 2019;9:11791.
37. Lee SY, Vuong TA, Wen X, et al. Methylation determines the extracellular calcium sensitivity of the leak channel NALCN in hippocampal dentate granule cells. *Exp Mol Med.* 2019;51:119.
38. Chua HC, Wulf M, Weidling C, Rasmussen LP, Pless SA. The NALCN channel complex is voltage sensitive and directly modulated by extracellular calcium. *Sci Adv.* 2020;6:eaa3154.
39. Biales B, Dichter MA, Tischler A. Sodium and calcium action potential in pituitary cells. *Nature.* 1977;267:172-174.
40. Tashjian AH Jr, Yasumura Y, Levine L, Sato GH, Parker ML. Establishment of clonal strains of rat pituitary tumor cells that secrete growth hormone. *Endocrinology.* 1968;82:342-352.
41. Tashjian AH Jr, Bancroft FC, Levine L. Production of both prolactin and growth hormone by clonal strains of rat pituitary tumor cells. Differential effects of hydrocortisone and tissue extracts. *J Cell Biol.* 1970;47:61-70.
42. Ostlund RE Jr, Leung JT, Hajek SV, Winokur T, Melman M. Acute stimulated hormone release from cultured GH3 pituitary cells. *Endocrinology.* 1978;103:1245-1252.
43. Ozawa S, Kimura N. Membrane potential changes caused by thyrotropin-releasing hormone in the clonal GH3 cell and their relationship to secretion of pituitary hormone. *Proc Natl Acad Sci USA.* 1979;76:6017-6020.
44. Lee JH, Cribbs LL, Perez-Reyes E. Cloning of a novel four repeat protein related to voltage-gated sodium and calcium channels. *FEBS Lett.* 1999;445:231-236.
45. Kschonsak M, Chua HC, Noland CL, et al. Structure of the human sodium leak channel NALCN. *Nature.* 2020;587:313-318.
46. Collu R, Lafond J, Marchisio AM, Eljarmak D, Ducharme JR. Sodium ions: their role and mechanism of action in the control of prolactin release. *Endocrinology.* 1984;114:1302-1307.
47. Reinl EL, Cabeza R, Gregory IA, Cahill AG, England SK. Sodium leak channel, non-selective contributes to the leak current in human

- myometrial smooth muscle cells from pregnant women. *Mol Hum Reprod.* 2015;21:816-824.
48. Lu B, Su Y, Das S, et al. Peptide neurotransmitters activate a cation channel complex of NALCN and UNC-80. *Nature.* 2009;457:741-744.
49. Chong JX, McMillin MJ, Shively KM, et al. De novo mutations in NALCN cause a syndrome characterized by congenital contractures of the limbs and face, hypotonia, and developmental delay. *Am J Hum Genet.* 2015;96:462-473.
50. Fujisawa S, Matsuki N, Ikegaya Y. Single neurons can induce phase transitions of cortical recurrent networks with multiple internal States. *Cereb Cortex.* 2006;16:639-654.

SUPPORTING INFORMATION

Additional Supporting Snformation may be found online in the Supporting Information section.

How to cite this article: Impheng H, Lemmers C, Bouasse M, et al. The sodium leak channel NALCN regulates cell excitability of pituitary endocrine cells. *The FASEB Journal.* 2021;35:e21400. <https://doi.org/10.1096/fj.202000841RR>